Liquid-Crystal Phase Reinforced Carbon Nanotube Fibers

Ranran Wang, Jing Sun,* and Lian Gao*

The State Key Lab of High Performance Ceramics and Superfine Microstructure, Shanghai Institute of Ceramics, Chinese Academy of Sciences, 1295 Ding Xi Road, Shanghai 200050, China

Received: January 5, 2010; Revised Manuscript Received: February 17, 2010

Fibers are promising forms to use carbon nanotubes (CNTs) on the macroscopic scale. Physical and chemical properties of carbon nanotubes, dispersants, and the phase behavior of carbon nanotube suspensions have great impact on the performance of the fibers. In this paper, single-walled carbon nanotube fibers were made by rotating PVA (poly(vinyl alcohol))-based coagulation spinning. Scanning electron microscopy was used to observe the surface and cross section of the fibers. The orientation degree of the fibers was analyzed by polarized Raman spectra. The influence of single-walled carbon nanotube (SWCNT) source materials and different dispersants on the performance of the fibers was investigated systematically for the first time. The results show that purification and acid oxidation of SWCNTs can enhance the fiber strength. Compared to SDS (sodium dodecyl sulfate) and SDBS (sodium dodecyl benzene sulfate), SLS (sodium lignosulfonate) is the best dispersant to fabricate carbon nanotube fibers with a higher strength. The performance of the fiber was improved greatly due to the formation of the liquid-crystal phase, and fibers with the strength of 520 MPa were fabricated.

1. Introduction

Carbon nanotubes (CNTs) have gained the interest of worldwide researchers due to their remarkable mechanical,[1] thermal,[2] and electrical properties.[3] There are a lot of applications of CNTs, such as composite material additives,[4] hydrogen storage,[5] biosensors,[6] and so on. Among these applications, composite reinforcement is one of the most important routes to utilize CNTs.[7−11] Unfortunately, the bad dispersion state and high suspension viscosity when the content of CNTs exceeded 10 wt % limit the contribution of CNTs to the performance of composite materials.[11] Therefore, new routes to utilize carbon nanotubes need to be developed. The concept of carbon nanotube fibers was put forward by Vigolo.[12] They are composed entirely,[13−17] or by a large fraction,[12,18,19] of aligned carbon nanotubes. Because of their high strength[20] and toughness,[21] carbon nanotube fibers can be woven into textile structures or used as cables and are among the most promising forms for using nanotubes on the macroscopic scale.[18]

Carbon nanotube fibers are usually prepared by the dry-spinning[13,15] or wet-spinning[18] process with water-based suspensions. PVA (poly(vinyl alcohol))-based coagulation spinning[12] is the most commonly used wet-spinning method. In this process, the carbon nanotube suspension is injected into a flowing solution of PVA. PVA molecules displace the dispersants and adsorb onto the tubes, causing coagulation of the fibers. A lot of work has been done to improve the strength of CNT fibers. For wet-spinning, the drawing treatment is an important and effective route to increase the strength of CNT fibers because drawing can improve the alignment of CNTs and polymer molecules. Poulin's group[18] and Dalton's group[19,21,22] have done a lot of work on the drawing treatment and increased the strength of CNT fibers significantly.

In addition to the drawing treatment, physicochemical properties of carbon nanotubes also have a great impact on the fiber performance. Besides, the dispersants, dispersion state, and phase behavior of CNT suspensions also play a significant role. However, there are few reports concentrated on these aspects to our knowledge. It is meaningful to investigate the influence of these factors on the fiber performance systematically.

Liquid-crystal solutions have been used to prepare fibers in order to achieve high orientation.[23] Some of the polymer fibers with the highest performance, such as Kevlar and PBO (poly(*p*-phenylene benzobisoxazole)), were produced by spinning from lyotropic liquid-crystal solutions of rigid-rod molecules. Similarly, CNTs can be viewed as high-aspect-ratio, rigid-rod molecules, and their liquid-crystalline phase can form at a certain condition. The liquid-crystalline behavior of CNT suspensions can offer a novel route to induce the alignment of CNTs. A number of studies have been performed investigating the liquid-crystal phase behavior of CNT suspensions.[24−29] Ericson[17] et al have spinned single-walled carbon nanotube (SWCNT) fibers from a lyotropic liquid-crystalline solution of SWCNTs, which were formed in fuming sulfuric acid, and the tensile strength of the fiber was about 116 MPa. However, CNTs used in their reports are too short to get a high fiber performance.

In our work, long SWCNTs (∼50 μm) were chosen to prepare fibers using the PVA-based coagulation spinning method. The influence of the SWCNT source materials, different types of dispersants, and phase behavior of SWCNT suspensions on fiber performance was investigated systematically. The SWCNT liquid-crystal phase formed when SLS was used as the dispersant, and the strength of the fibers was greatly improved by spinning from liquid-crystalline solutions of SWCNTs.

2. Experimental Methods

Chemicals. The SWCNTs prepared by the CVD (chemical vapor deposition) method were bought from the Chengdu Organic Chemicals Co. Ltd., Chinese Academy of Sciences. Their length was about 50 μm and the diameters were about

* To whom correspondence should be addressed. Tel: +86-21-52412718 (L.G.). Fax: +86-21-52413122. E-mail: jingsun@mail.sic.ac.cn (J.S.), liangaoc@online.sh.cn (L.G.).

10.1021/jp100108m
Published on Web 03/03/2010

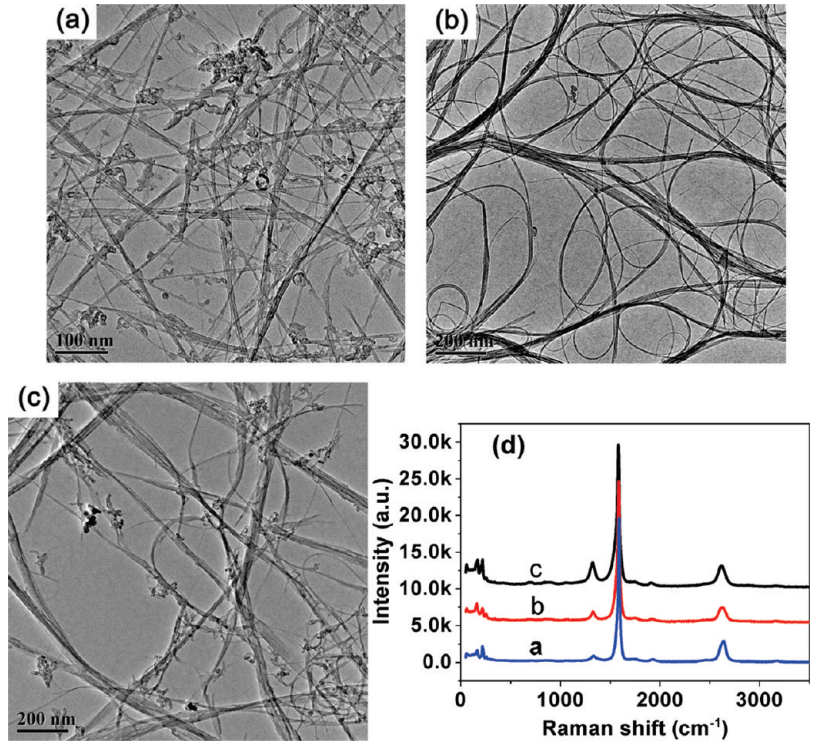

Figure 1. TEM images of pristine (a), purified (b), and acid-oxidized SWCNTs (c). (d) Raman spectra of SWCNTs: a, pristine; b, purified; c, acid-oxidized.

1−2 nm. SDS (sodium dodecyl sulfate) was purchased from Shanghai Chemical Reagent Company. Poly(vinyl alcohol) (PVA, MW ∼120K, alcoholysis ≥ 93.0%) and SDBS (sodium dodecyl benzene sulfate) were provided by Sinopharm Chemical Reagent Co., Ltd. Sodium lignosulfonate (SLS, MW ∼30K) was purchased from R. T. Vanderbilt Company, Inc.

Purification of SWCNTs. An efficient and nondestructive approach reported by Ma et al[30] was used to purify SWCNTs. Pristine SWCNTs were kept at 400 °C in air for 1 h and then heat-treated at 900 °C for 1 h under the protection of N_2. After that, the sample was refluxed in 12 M hydrochloric acid at 100 °C for 4 h. The sample was then filtered through a 0.22 μm Millipore polypropylene membrane and was rinsed with distilled water until the filtrate became neutral. The obtained cake was finally dried at 60 °C.

Acid Oxidation of SWCNTs. SWCNTs (1 g) were refluxed in 100 mL of 15 M HNO_3 at 140 °C for 6 h and then were rinsed with distilled water until the filtrate became neutral. The sample was then rinsed once with some ethanol. The obtained cake was finally dried at 60 °C.

Fiber Preparation. PVA-based coagulation spinning developed by Vigolo[12] was used to prepare SWCNT fibers. SWCNT suspensions were fabricated by dispersing SWCNTs in SDS or SDBS or SLS aqueous solution and then homogenizing with a horn sonicator (XL2007, Misonix Incorporated) for 60 min with a power of 100 W. PVA aqueous solution with the concentration of 3 wt % was used as the coagulating medium. The SWCNT suspension went through the capillaries that were 25 cm long with the diameter of 0.625 mm and then was injected into a rotating coagulation bath at the rate of 60 mL/h. The rotation rate of the coagulation bath was 30 rpm. After spinning, the coagulation bath was kept still until the obtained CNT ribbons sank to the bottom. The PVA solution was then decanted, and CNT ribbons were rinsed with a large amount of water. At last, the ribbons were drawn out and dried under tension.

Characterization. The morphology of SWCNTs subjected to different treatments was observed by transmission electron microscopy (TEM, JEM-2100F, JEOL, Tokyo, Japan). Raman spectra of SWCNT powders were recorded using a Renishaw MicroRaman spectrometer with an excitation length of 633 nm. The absorption spectra of SWCNT suspensions were measured via a UV−vis spectrometer (Lambda 950, PerkinElmer, Shelton, U.S.A.). The surface morphology and the broken end of the fibers were characterized by a field emission scanning electron microscope (FESEM, JEOL, JSM-6700F). Mechanical properties of the fibers were measured by an XQ-1 fiber strength instrument. The strength of each fiber was measured five times, and the average data were recorded. These radii of the fibers were measured by an optical microscope (BM-12, Shanghai Optical Instrument). A polarized optical microscope (IEB-237, Carl Zeiss, Jena, Germany) was used to take crossed-polarized images of SWCNT suspensions.

3. Results and Discussion

3.1. Influence of SWCNT Modifications. In our experiment, pristine, purified, and acid-oxidized SWCNTs were chosen as raw materials to fabricate fibers under the same experimental conditions. Figure 1a shows that a lot of impurities existed in pristine SWCNT powders, including catalyst particles and amorphous carbon. From Figure 1b,c, it can be seen that most of the impurities were removed after purification and acid oxidation. Raman spectra showed that the I_D/I_G ratio decreased after purification and acid oxidation, again indicating the removal of impurities.[30] Although acid oxidation induced some defects and carboxyl groups on the side wall,[31,32] no significant damage on the wall structure of SWCNTs was observed in our experiments, as estimated from Raman spectra in Figure 1d.

Table 1 shows that the strength of the fiber was enhanced for the purified and the acid-oxidized ones. Fibers prepared with acid-oxidized SWCNTs had the highest strength. These phe-

TABLE 1: Influence of Three Types of SWCNTs on the Fiber Performance

SWCNT	concentration of SWCNTs (wt %)	dispersants	concentration of dispersants (wt %)	tensile strength (Mpa)	strain to failure (%)
1 pristine	0.35	SDS	1	132	10.32
2 purified	0.35	SDS	1	211	18.5
3 acid-oxidized	0.35	SDS	1	300	3.4

nomena can be rationalized by considering three factors: (1) Removal of impurity particles can enhance compactness and interfacial adhesion between SWCNTs themselves and SWCNTs with PVA. This is beneficial to the load transfer from SWCNTs to PVA and from one SWCNT−PVA composite bundle to another. The fiber prepared with purified SWCNTs was more compact, as seen from SEM images of the fibers (Figure 2), resulting in better load transfer and higher strength. (2) Carboxyl groups of SWCNTs induced by acid oxidation can form hydrogen bonds or even covalent bonds with hydroxyl groups on PVA. Both types of bonds are stronger than van der Waals interactions and can lead to better stress transfer between SWCNTs and PVA.[33] (3) A better dispersion state was obtained because hydrophilic groups, such as −COOH and −OH, were induced onto the tubes in the acid oxidation process. UV−vis spectra and an optical microscope were used to characterize the dispersion state of SWCNTs. As shown in the UV−vis spectra in Figure 3a, the absorbance value of the acid-oxidized SWCNT suspension at 288 nm was much higher than that of pristine SWCNTs, indicating a stable and higher concentration of suspended SWCNTs.[34−37] The phenomenon was also observed intuitively by optical microscope images shown in Figure 3. Carbon nanotubes that are in less aggregated states will improve the performance of the fibers, according to a previous report[18] and our own experiments.

3.2. Different Dispersants and Liquid-Crystal Phase Formation. Table 2 shows that the performance of the fibers reaches the highest value when SLS was used as dispersant. Although SDBS showed the best dispersion ability among the three dispersants, according to the UV−vis spectrum, the corresponding fiber had the lowest tensile strength. This may be due to strong interaction between SDBS and SWCNTs. In the process of SWCNT fiber formation, PVA adsorbs onto the tubes and displaces some dispersant molecules, leading to the aggregation of SWCNTs.[12] However, strong interaction between SDBS and SWCNTs hindered the displacement of SDBS by PVA and led to weak interaction between SWCNTs and PVA. Therefore, the newly formed fiber was easily redispersed when disturbed, and it was difficult to obtain a continuous fiber. These findings indicated that a better dispersion state did not necessarily lead to high fiber performance. Whether the dispersant can be easily displaced in the coagulation process is also crucial because it will influence the interaction between CNTs and coagulation bath molecules and the continuous formation of fibers. The ability to facilitate continuous fiber formation was defined as fiber formation ability here. It came out that dispersion ability and fiber formation ability are two important factors of dispersants we should consider when they are used to prepare CNT fibers. SLS and SDS are superior to SDBS in view of these two factors. Not only can they disperse SWCNTs into small bundles but also they can be easily displaced. Therefore, the fibers prepared with the two dispersants had better performance. When the concentration of the SWCNTs was increased to 0.5 wt %, the strength of fibers prepared from the SWCNT−SLS suspension was enhanced a lot, whereas that of fibers prepared from the SWCNT−SDS suspension was enhanced only a little. At first, we contribute the improvement to a better dispersion state. However, there is no big difference between the absorption intensity of the SWCNT−SLS suspension and SWCNT−SDS suspension seen from UV−vis spectra (Figure 4), indicating a similar dispersion state of SWCNTs. The difference between them may be attributed to the formation of the liquid-crystal phase in SWCNT−SLS suspensions, which will be discussed in the following part.

Some researchers[28,38,39] have reported that the liquid-crystal phase can form when the concentration of CNTs is elevated to a certain value. It was deduced that the liquid-crystal phase formed in the SWCNT (0.5 wt %)−SLS (1 wt %) suspension and improved the alignment of carbon nanotubes in the fibers. A polarized optical microscope was used to prove this conjecture. After a few hours of sonication, a small droplet of the SWCNT (0.5 wt %)−SLS (1 wt %) suspension was dropped on a piece of clean glass slide and optical images were taken under crossed-polar illumination. Some bright regions observed in the crossed-polarized images indicated the formation of the lyotropic liquid-crystal phase.[40] In contrast, this phenomenon was not observed in the crossed-polarized images of the SWCNT (0.5 wt %)−SDS (1 wt %) suspension. Figure 5 shows crossed-polarized images of the SWCNT (0.5 wt %)−SLS (1 wt %) suspension taken at 0 and 8 h after sonication. We found that phase transition (from the disordered to the ordered) of the SWCNT (0.5 wt %)−SLS (1 wt %) suspension occurred a few hours after sonication. SEM image revealed the alignment of SWCNTs in the liquid-crystal phase (Figure 5c). Some aligned regions were also observed in TEM images of the SWCNT (0.5 wt %)−SLS (1 wt %) suspension, as shown in Figure 5d. When the concentration of the SWCNTs was elevated to 0.7 wt %, the liquid-crystal phase of the SWCNT−SLS suspension disappeared due to the bad dispersion state.

The degree of the alignment of nanotubes was also characterized by polarized Raman spectra. Data in VV (vertical vertical) polarization are presented in Figure 6 with an excitation length of 633 nm. The angle between the fiber axis and light polarization direction is called ψ here. From Figure 6, the maximum intensity of the G peak was observed at $\psi = 20°$ and it decreased continuously from $\psi = 20°$ to $\psi = 100°$. Similar dependence can be observed in both the D-peak and the RBM (radical breathing mode) region. This dependence behavior proves the alignment of SWCNTs in the fiber. The intensity ratio (maximum/minimum) can be used to qualify the orientation degree of CNTs in fibers.[41] The higher the ratio, the better the orientation degree. Here, Ivv20/Ivv100 is used to qualify the orientation degree of SWCNTs in different fibers. The intensity ratio of fibers prepared from the 0.5 wt % SWCNT suspension increased from 4.6 to 7.2 when the dispersant was changed from SDS to SLS. The ratio increased from 4.6 to 5.3 when the laser focused deep into a fiber, indicating better alignment of SWCNTs in the interior part of the fiber than on the surface. Anglaret et al.[42] ever reported that the intensity of the G peak and RBM was maximal when ψ was 0° and was minimal when ψ was 90°. The deviation between our results and the report may be ascribed to two reasons: (1) Parallax existed in the process of setting the initial direction of the fibers by the naked eye. A fiber was put along the y axis, which is parallel with the initial light polarization direction. However, some deviation may be induced due to parallax. That means that the actual angle between the fiber axis and the light polarization direction deviated from the ψ we set. (2) The orientation of the nanotubes was not exactly consistent with the fiber axis. There may be a small angle between them.

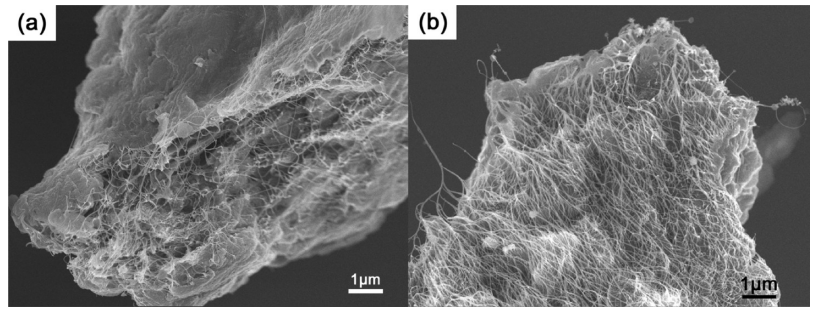

Figure 2. SEM images of (a) a pristine SWNT fiber and (b) a purified SWNT fiber.

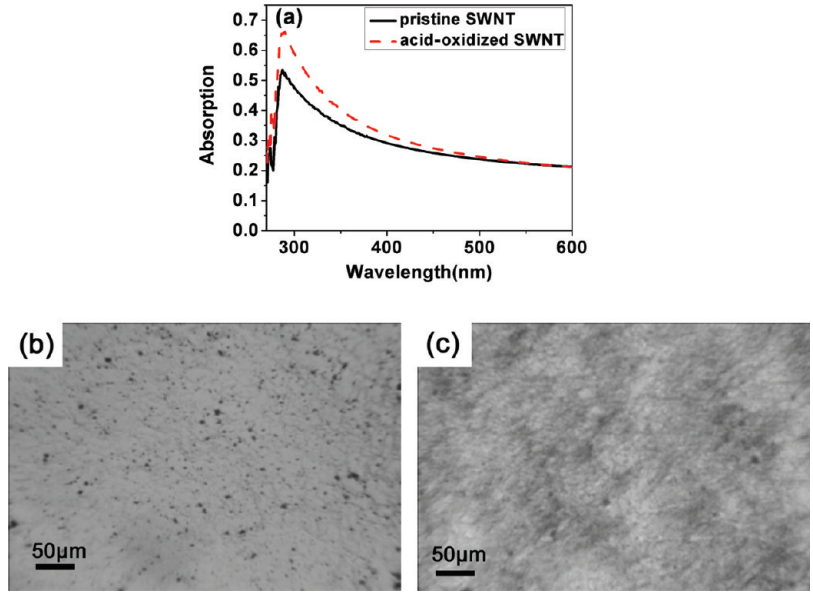

Figure 3. (a) UV−vis spectra of SWCNT suspensions. Optical microscope images of pristine (b) and acid-oxidized SWCNT suspensions (c).

TABLE 2: Influence of Three Types of Dispersants on the Fiber Performance

SWCNT	concentration of SWCNTs (wt %)	dispersants	concentration of dispersants (wt %)	tensile strength (Mpa)	strain to failure (%)
1 acid-oxidized	0.35	SDS	1	300	3.4
2 acid-oxidized	0.35	SDBS	1	253	3.4
3 acid-oxidized	0.35	SLS	1	353	3.6
4 acid-oxidized	0.5	SDS	1	330	1.6
5 acid-oxidized	0.5	SLS	1	520	3.26

Onsager[43] predicted that the rod−solvent system formed an anisotropic liquid-crystalline phase at concentrations above $C_2 \approx 3.3\rho d/l$, where ρ was the mass density and d/l was the rod aspect ratio. In the present study, the sizes of most bundles are between 10 and 20 nm in the SWCNT (0.5 wt %) suspension, according to TEM images. The density of the SWCNTs is 2.1 g/cm^3. According to the equation, we can estimate that the length of SWCNTs after sonication was about 14−28 μm. That means that the nanotubes were shortened after sonication. However, they are still very long compared with SWCNTs used to form the liquid-crystalline phase in other studies.[24−28] No liquid-crystal phase was observed in the SWCNT−SDS suspension at the same concentration. Two points are brought up to explain this phenomenon. First, the phase transition of the SWCNT suspension can be promoted by SLS. SLS is a macromolecule that has rigid phenyl groups and flexible C−O and C−C chains. This kind of macromolecule is inclined to align ordered when the concentration of the solution is high.[44] Therefore, the adsorption of SLS may induce the interactions between SWCNTs. These interactions can modify the phase diagram and the phase boundaries of the system. The transition from an isotropic phase to a nematic phase will be shifted to small volume fractions if the nanotubes interact. Second, as macromolecules, SLS increased the viscosity of the SWCNT suspension, which can hinder the sediment of SWCNTs. In the present work, SWCNTs in concentrated suspensions subsided easily because they were long and hard to disperse. High viscosity can slow this process and keep a high concentration of the SWCNT suspension. SWCNTs dispersed in SDS precipitated faster because the viscosity is low. However, phase transition needs time. The concentration of the SWCNT−SDS system may have decreased to a value below C_2 before phase transition starts. Therefore, the liquid-crystal phase was not observed in the SWCNT−SDS system.

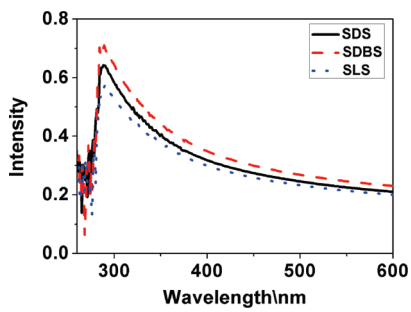

Figure 4. UV−vis spectra of SWCNT suspensions.

The ordered phase, in contrast to the isotropic phase is beneficial to the alignment of SWCNTs in fibers. The strength

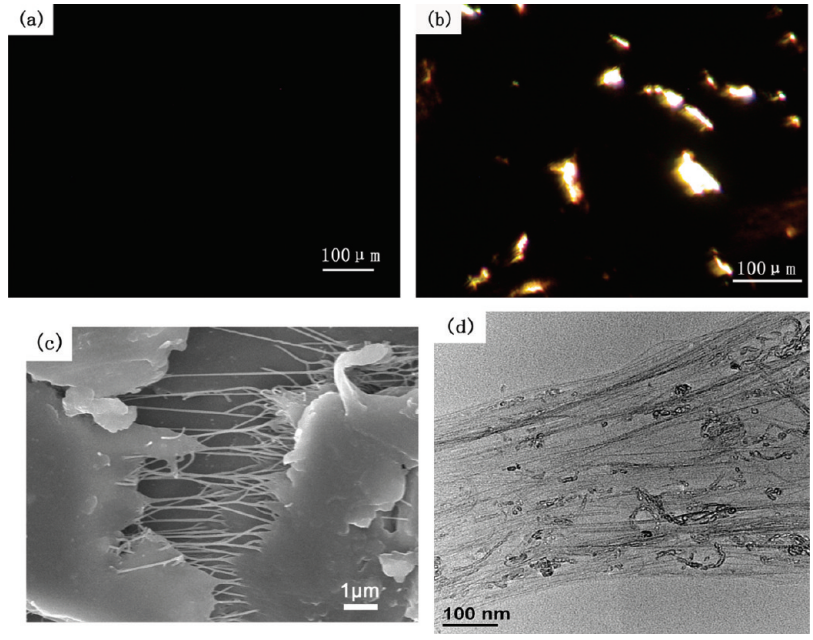

Figure 5. Polarized optical images of SWCNT (0.5 wt %)−SLS(1 wt %) suspensions taken at 0 (a) and 8 h (b) after sonication. (c) SEM image of sample (b). (d) TEM image of sample (b).

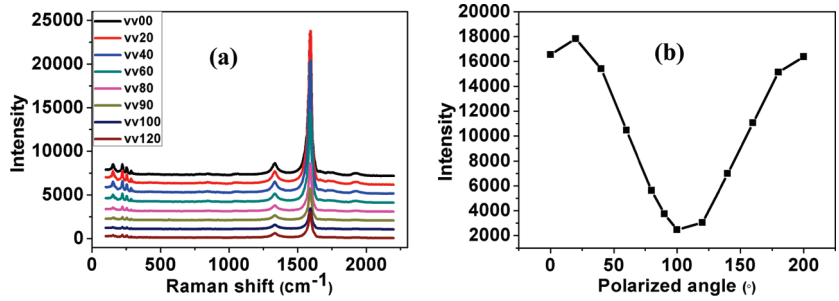

Figure 6. (a) Polarized Raman spectra of SWCNT fibers, from top to bottom: $\psi = 0°$, 20°, 40°, 60°, 80°, 90°, 100°, and 120°. (b) Intensity change of the G band with ψ.

of fibers will be enhanced by improving the orientation of carbon nanotubes. Therefore, it is meaningful to investigate CNT liquid-crystal solutions that can offer a novel route to induce the alignment of CNTs. A number of studies have investigated the liquid-crystal phase behavior of CNT dispersions.[24−28,38,40] However, CNTs used in these reports are short, from several hundred nanometers to several micrometers. CNTs with a high aspect ratio are beneficial to load transfer,[29] which means that the strength of SWCNT fibers can be enhanced by using long SWCNTs. Therefore, the liquid-crystal phase of long SWCNTs is of great importance for fabricating CNT fibers with high strength. To our knowledge, it is the first time to investigate the liquid-crystal phase behavior of such long SWCNTs and prepare fibers with this SWCNT liquid-crystal solution.

4. Conclusions

We have investigated the influence of SWCNT source materials on the performance of CNT fibers and found that purified SWCNTs enhanced the strength of the fibers, which was mainly attributed to densification of the fiber. The strength can be enhanced further by using acid-oxidized SWCNTs as raw materials because of the better dispersion state and the formation of hydrogen bonds between SWCNTs and PVA. Dispersants also had great impact on the performance of the fibers. In addition to their dispersion ability, whether they can be easily displaced in the coagulation process is also crucial because it will influence the interaction between CNTs and coagulation bath molecules and the continuous formation of fibers. SLS and SDS are better than SDBS in view of these two factors. The liquid-crystal phase was observed in the SWCNT−SLS suspension when the concentration of SWCNTs was elevated to 0.5 wt %. The fiber performance was improved a lot by using these ordered SWCNT solutions.

Acknowledgment. This work was financially supported by the Shanghai Talents Program Foundation, the National Key Basic Research Development Program of China (2005CB623605), and the National Nature Science Foundation of China (50972153). We appreciate the help from Prof. Q. H. Zhang for mechanical measurements.

References and Notes

(1) Coleman, J. N.; Khan, U.; Gun'ko, Y. K. *Adv. Mater.* **2006**, *18*, 689–706.
(2) Berber, S.; Kwon, Y. K.; Tomanek, D. *Phys. Rev. Lett.* **2000**, *84*, 4613–4616.
(3) Wei, B. Q.; Vajtai, R.; Ajayan, P. M. *Appl. Phys. Lett.* **2001**, *79*, 1172–1174.
(4) Zhu, J.; Kim, J. D.; Peng, H. Q.; Margrave, J. L.; Khabashesku, V. N.; Barrera, E. V. *Nano Lett.* **2003**, *3*, 1107–1113.
(5) Iyakutti, K.; Kawazoe, Y.; Rajarajeswari, M.; Surya, V. J. *Int. J. Hydrogen Energy* **2009**, *34*, 370–375.
(6) Claussen, J. C.; Franklin, A. D.; ul Haque, A.; Porterfield, D. M.; Fisher, T. S. *ACS Nano* **2009**, *3*, 37–44.

(7) Baughman, R. H.; Zakhidov, A. A.; de Heer, W. A. *Science* **2002**, *297*, 787–792.
(8) Biercuk, M. J.; Llaguno, M. C.; Radosavljevic, M.; Hyun, J. K.; Johnson, A. T.; Fischer, J. E. *Appl. Phys. Lett.* **2002**, *80*, 2767–2769.
(9) Coleman, J. N.; Blau, W. J.; Dalton, A. B.; Munoz, E.; Collins, S.; Kim, B. G.; Razal, J.; Selvidge, M.; Vieiro, G.; Baughman, R. H. *Appl. Phys. Lett.* **2003**, *82*, 1682–1684.
(10) Sreekumar, T. V.; Liu, T.; Min, B. G.; Guo, H.; Kumar, S.; Hauge, R. H.; Smalley, R. E. *Adv. Mater.* **2004**, *16*, 58.
(11) Munoz, E.; Suh, D. S.; Collins, S.; Selvidge, M.; Dalton, A. B.; Kim, B. G.; Razal, J. M.; Ussery, G.; Rinzler, A. G.; Martinez, M. T.; et al. *Adv. Mater.* **2005**, *17*, 1064–1067.
(12) Vigolo, B.; Penicaud, A.; Coulon, C.; Sauder, C.; Pailler, R.; Journet, C.; Bernier, P.; Poulin, P. *Science* **2000**, *290*, 1331–1334.
(13) Zhang, M.; Atkinson, K. R.; Baughman, R. H. *Science* **2004**, *306*, 1358–1361.
(14) Koziol, K.; Vilatela, J.; Moisala, A.; Motta, M.; Cunniff, P.; Sennett, M.; Windle, A. *Science* **2007**, *318*, 1892–1895.
(15) Li, Y. L.; Kinloch, I. A.; Windle, A. H. *Science* **2004**, *304*, 276–278.
(16) Li, Q. W.; Zhang, X. F.; DePaula, R. F.; Zheng, L. X.; Zhao, Y. H.; Stan, L.; Holesinger, T. G.; Arendt, P. N.; Peterson, D. E.; Zhu, Y. T. *Adv. Mater.* **2006**, *18*, 3160–3163.
(17) Ericson, L. M.; Fan, H.; Peng, H. Q.; Davis, V. A.; Zhou, W.; Sulpizio, J.; Wang, Y. H.; Booker, R.; Vavro, J.; Guthy, C.; et al. *Science* **2004**, *305*, 1447–1450.
(18) Miaudet, P.; Badaire, S.; Maugey, M.; Derre, A.; Pichot, V.; Launois, P.; Poulin, P.; Zakri, C. *Nano Lett.* **2005**, *5*, 2212–2215.
(19) Dalton, A. B.; Collins, S.; Razal, J.; Munoz, E.; Ebron, V. H.; Kim, B. G.; Coleman, J. N.; Ferraris, J. P.; Baughman, R. H. *J. Mater. Chem.* **2004**, *14*, 1–3.
(20) Zhang, X. F.; Li, Q. W.; Holesinger, T. G.; Arendt, P. N.; Huang, J. Y.; Kirven, P. D.; Clapp, T. G.; DePaula, R. F.; Liao, X. Z.; Zhao, Y. H.; et al. *Adv. Mater.* **2007**, *19*, 4198–4201.
(21) Dalton, A. B.; Collins, S.; Munoz, E.; Razal, J. M.; Ebron, V. H.; Ferraris, J. P.; Coleman, J. N.; Kim, B. G.; Baughman, R. H. *Nature* **2003**, *423*, 703–703.
(22) Razal, J. M.; Coleman, J. N.; Munoz, E.; Lund, B.; Gogotsi, Y.; Ye, H.; Collins, S.; Dalton, A. B.; Baughman, R. H. *Adv. Funct. Mater.* **2007**, *17*, 2918–2924.
(23) Afshari, M.; Sikkema, D. J.; Lee, K.; Bogle, M. *Polym. Rev.* **2008**, *48*, 230–274.
(24) Basu, R.; Iannacchione, G. S. *Appl. Phys. Lett.* **2008**, *93*, 183105.
(25) Kordas, K.; Mustonen, T.; Toth, G.; Vahakangas, J.; Uusimaki, A.; Jantunen, H.; Gupta, A.; Rao, K. V.; Vajtai, R.; Ajayan, P. M. *Chem. Mater.* **2007**, *19*, 787–791.
(26) Lynch, M. D.; Patrick, D. L. *Nano Lett.* **2002**, *2*, 1197–1201.
(27) Dierking, I.; Scalia, G.; Morales, P.; Leclere, D. *Adv. Mater.* **2004**, *16*, 865–869.
(28) Song, W. H.; Kinloch, I. A.; Windle, A. H. *Science* **2003**, *302*, 1363–1363.
(29) Liu, K.; Sun, Y. H.; Chen, L.; Feng, C.; Feng, X. F.; Jiang, K. L.; Zhao, Y. G.; Fan, S. S. *Nano Lett.* **2008**, *8*, 700–705.
(30) Ma, J.; Wang, J. N. *Chem. Mater.* **2008**, *20*, 2895–2902.
(31) Zhang, J.; Zou, H. L.; Qing, Q.; Yang, Y. L.; Li, Q. W.; Liu, Z. F.; Guo, X. Y.; Du, Z. L. *J. Phys. Chem. B* **2003**, *107*, 3712–3718.
(32) Liu, J.; Rinzler, A. G.; Dai, H. J.; Hafner, J. H.; Bradley, R. K.; Boul, P. J.; Lu, A.; Iverson, T.; Shelimov, K.; Huffman, C. B.; et al. *Science* **1998**, *280*, 1253–1256.
(33) Lachman, N.; Bartholome, C.; Miaudet, P.; Maugey, M.; Poulin, P.; Wagner, H. D. *J. Phys. Chem. C* **2009**, *113*, 4751–4754.
(34) Yu, J. R.; Grossiord, N.; Koning, C. E.; Loos, J. *Carbon* **2007**, *45*, 618–623.
(35) Li, Z. F.; Luo, G. H.; Zhou, W. P.; Wei, F.; Xiang, R.; Liu, Y. P. *Nanotechnology* **2006**, *17*, 3692–3698.
(36) Liu, Y. Q.; Gao, L.; Zheng, S.; Wang, Y.; Sun, J.; Kajiura, H.; Li, Y.; Noda, K. *Nanotechnology* **2007**, *18*, 365702.
(37) Jiang, L. Q.; Gao, L.; Sun, J. *J. Colloid Interface Sci.* **2003**, *260*, 89–94.
(38) Moulton, S. E.; Maugey, M.; Poulin, P.; Wallace, G. G. *J. Am. Chem. Soc.* **2007**, *129*, 9452–9457.
(39) Badaire, S.; Zakri, C.; Maugey, M.; Derre, A.; Barisci, J. N.; Wallace, G.; Poulin, P. *Adv. Mater.* **2005**, *17*, 1673–1676.
(40) Bergin, S. D.; Nicolosi, V.; Giordani, S.; de Gromard, A.; Carpenter, L.; Blau, W. J.; Coleman, J. N. *Nanotechnology* **2007**, *18*, 455705.
(41) Fischer, D.; Potschke, P.; Brunig, H.; Janke, A. *Macromol. Symp.* **2005**, *230*, 167–172.
(42) Anglaret, E.; Righi, A.; Sauvajol, J. L.; Bernier, P.; Vigolo, B.; Poulin, P. *Phys. B* **2002**, *323*, 38–43.
(43) Sabba, Y.; Thomas, E. L. *Macromolecules* **2004**, *37*, 4815–4820.
(44) Wilson, M. R. *Int. Rev. Phys. Chem.* **2005**, *24*, 421–455.

JP100108M